

We are IntechOpen, the world's leading publisher of Open Access books Built by scientists, for scientists

6,900

Open access books available

186,000

International authors and editors

200M

Downloads

Our authors are among the

154

Countries delivered to

TOP 1%

most cited scientists

12.2%

Contributors from top 500 universities



WEB OF SCIENCE™

Selection of our books indexed in the Book Citation Index
in Web of Science™ Core Collection (BKCI)

Interested in publishing with us?
Contact book.department@intechopen.com

Numbers displayed above are based on latest data collected.
For more information visit www.intechopen.com



Nonlinear Predictive Control of Semi-Active Landing Gear

Dongsu Wu, Hongbin Gu and Hui Liu
*Nanjing University of Aeronautics and Astronautics
China*

1. Introduction

When airplane touches down and taxis on uneven runways with high speed, there is heavy ground impact and huge vertical load to the airframe. To improve safety and make passengers comfortable during landing, an effective landing gear capable of absorbing impact energy as much as possible is indispensable for modern airplane. Besides the basic function of reducing impact loads, the landing gear must also allow sufficient maneuverability during ground operation, which leads to conflicting requirements in terms of the suspension system (Krüger, 2000). Traditional landing gear consists of tires and passive shock absorbers, which can only be optimized before leaving factory to ensure the landing gear having a fairly good performance in particular design operational conditions, typically hard landings. However, due to its fixed structure, the passive shock absorber cannot always work well on various ground conditions and operational conditions. A heavy landing or a coarse runway may lead to significant deterioration of its performance, which is harmful to the fatigue life of the landing gear and of the airframe.

Active control and semi-active control are widely used approach in the field of construction vibration control and vehicle suspension control. Compared with passive control, active and semi-active control has excellent tunable ability due to their flexible structure. Active control needs an external hydraulic source to supply energy for the system. The main drawback of active control approach is that its structure is very complex and the external energy may lead to instability of the system. The semi-active approach (Fig.1) modifies the damping characteristics by changing the size of the orifice area and does not introduce any external energy. Studies by Karnopp (Karnopp, 1983) for automotive applications also suggest that the efficiency of semi-active dampers is only marginally lower than of a fully active system, provided that a suitable control concept is used. In consideration of its simple structure and high reliability, semi-active control approach could be a better choice for landing gear systems.

The main component of semi-active landing gear system is a tunable oleo-pneumatic shock absorber, which contains multidisciplinary and highly nonlinear dynamics. It is not an easy task to design an effective controller for such complex system. Krüger (Krüger, 2000) focuses his studies on optimization of taxiing performance of a semi-active landing gear. SIMPACK software is used to run simulation with a complete aircraft FEA model. Ghiringhelli builds a

complete aircraft landing simulation model in ADAMS software (Ghiringhelli et al., 2004). A semi-active PID control method is used to control the orifice area. His also studies sensitivity of the complete aircraft model to the variation of control parameters and compares the results obtained in the simulated drop tests between passive and semi-active approach (Ghiringhelli, 2000). Maemori et al. (Maemori et al., 2003) proposes an optimization method for a semi-active landing gear to handle variations in the maximum vertical acceleration of an aircraft during landing caused by the variation of the aircraft mass, which is always due to the variations in the number of passengers, and the amounts of cargo and fuel. Wang et al. (Wang et al., 1999) considers both taxiing and landing conditions. He uses a fuzzy controller to optimize the performance of the semi-active landing gear. But he does not consider the dynamics of the actuator. Mikulowski et al. (Mikulowski et al., 2008) discuss the application of piezo-actuators and magneto-rheological damper in the adaptive landing gear design. And there are some other researchers applying ER (Lou et al., 1993) or MR (Batterbee et al., 2007) technology in semi-active land gear system. All of the semi-active controllers designed above do not consider the actuator saturations (limited control amplitude and rate), which may lead to significant, undesirable deterioration in the closed-loop performance and even closed-loop instability.

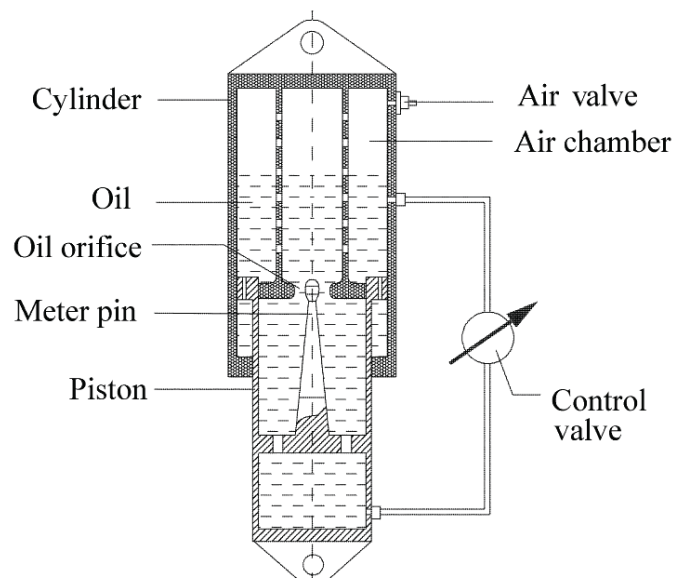


Fig. 1. Structure of Semi-Active Controlled Shock Absorber

Model predictive control refers to a class of control algorithms in which a dynamic model is used to predict and optimize control performance. The predictions are obtained from a dynamic model and the optimization problem is solved subject to constraints on input and output variables. So MPC is especially suited for constrained, digital control problems. Initially MPC has been widely used in the industrial processes with linear models, but recently some researchers have tried to apply MPC to other fields like automotive (Mehra et al., 1997) and aerospace (Hyochoong et al., 2004), and the nonlinear model is used instead of linear one due to the increasingly high demands on better control performance and rapidly developed powerful computing systems (Michael et al., 1998). To the semi-active landing gear control problem, the nonlinear model predictive control is a good choice considering its effectiveness to constrained control problems and continuously optimized performance. The goal of this paper is to introduce the design and the analysis of a nonlinear hierarchical

control strategy, for semi-active landing gear systems in civil and military aircrafts, based on predictive control strategies.

2. Dynamic Model of Semi-Active Landing Gear

The structure mass of landing gear is divided into sprung mass and non-sprung mass. Sprung mass defined in the figure includes the airframe, the cylinder etc. Non-sprung mass includes the piston rod, wheel etc. The tire is modelled as a simple spring and the tunable damping is realized by a variable size orifice which is controlled by a high-speed solenoid valve.

The governing dynamic equations of semi-active landing gear can be presented as the following:

$$m_s \ddot{z}_s = m_s g - F \tag{1}$$

$$m_u \ddot{z}_u = m_u g + F - P \tag{2}$$

Where m_u is the unsprung mass, m_s the sprung mass, z_u the displacement of unsprung part, z_s the displacement of sprung part, P the vertical force on the tire, F the semi-active damper shock strut force.

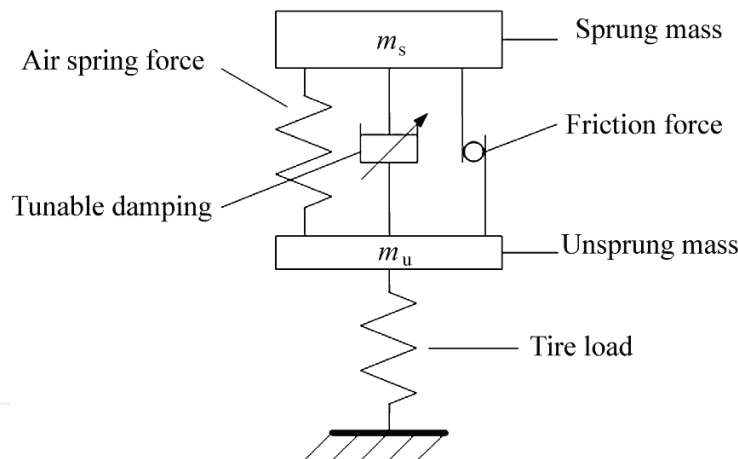


Fig. 2. System Model of Semi-Active Landing Gear

2.1 Shock Strut Force Model

Considering basics of the shock strut operation, a damping effect is produced by squeezing the compressed oil through the tunable orifice. In the pneumatic chamber, the enclosed air is compressed by the movement of the piston, which provides an air cushion spring. There is also friction produced between sliding parts. All these forces comprise the shock strut force (Yadav et al., 1991):

Oleo damping force:

$$F_{oil} = \frac{\rho A_o^3 \operatorname{sgn}(\dot{z}_s - \dot{z}_u)}{2(A_d C_d)^2 \sqrt{1 - (A_d / A_o)^2}} (\dot{z}_s - \dot{z}_u)^2 \tag{3}$$

Air spring force:

$$F_{air} = P_i A_a \left[\frac{V_0}{V_0 - A_a (z_s - z_u)} \right]^n - P_0 A_a \quad (4)$$

Friction force:

$$F_f = K_m F_{air} \quad (5)$$

Total axial force in the shock strut:

$$F = F_{air} + F_f + F_{oil} \quad (6)$$

where ρ is the oil density, P_i is the initial pneumatic pressure of air chamber, P_0 is the atmospheric pressure, A_0 is the effective oil action area, A_a is the effective air action area, A_d is the tunable oil orifice area, C_d is the tunable oil orifice flow coefficient, V_0 is the initial volume of air chamber, K_m is the coefficient of kinetic friction.

2.2 Tire Force Model

The vertical force P on the tire is due to polytropic compression of air inside the tire. In order to simplify the mathematical model, the tire is treated as a linear spring here:

$$P = K_t z_u + C_t \dot{z}_u \quad (7)$$

where K_t is the stiffness coefficient of tire, and C_t the damp coefficient of tire.

2.3 Model of High Speed Solenoid Valve

Traditional solenoid valve (Fig.3) are simple in construction, rugged, relatively cheap to produce and have higher power-mass ratio, but they are not usually used for continuous and proportional control due to its high nonlinearity. Recently, some attempts are made in this kind of application using nonlinear control methods. According to our previous studies (Liu H. et al, 2008), we model a high speed solenoid valve by considering its mechanical, magnetic and electrical dynamics.

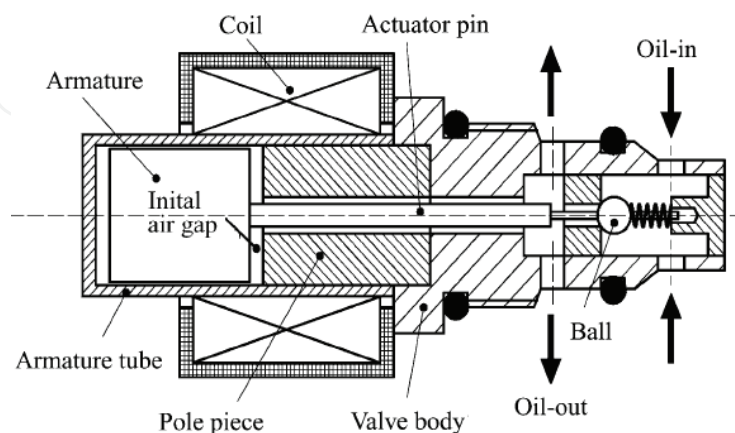


Fig. 3. High-speed Solenoid Valve's Structure

(a) The mechanical dynamics of solenoid valve can be expressed as below:

$$m_v \ddot{x}_v + C_s \dot{x}_v + (K_s + K_f)x_v + f_0 + f = F_v \quad (8)$$

where m_v is the total mass of movable parts including armature, actuator pin, etc., C_s viscous damping coefficient, K_s spring stiffness, K_f static flow coefficient, f_0 preloading force of spring, f Coulomb friction, and x_v movable part displacement and is proportional to oil orifice area A_d .

$$A_d = K_v x_v \quad (9)$$

where K_v is the proportionality coefficient.

(b) The magnetic dynamics of solenoid valve can be summarized as following:

The magnetomotive force is

$$\mathcal{E}_m = Ni = \Phi R_m \quad (10)$$

where N is the coil turns, i current, R_m total magnetic reluctance, and Φ total magnetic flux.

The electromagnetic force that acts on the armature of valve can be given by

$$F_v = \frac{\Phi_{air}^2}{2\pi\mu_0 r^2 \lambda^2} \quad (11)$$

where μ_0 is the air permeability, r the radius of armature, λ the leakage coefficient of the main air gap, and Φ_{air} magnetic flux passing through the working air gap.

$$\Phi_{air} = \frac{R_o R_L}{R_o + R_L} \Phi \quad (12)$$

R_o and R_L are corresponding to the magnetic reluctance of two part of magnetic flux paths. Due to the fact that λ , R_o , R_L , R_m are related to x_v , and according to Eq. (10-12), the magnetic equations of solenoid valve can be simplified as:

$$F_v = B(x_v) i^2 \quad (13)$$

where $B(x_v)$ is a function of x_v and represents nonlinear magnetic dynamics of valve. F_v depends on i^2 , the square of electrical current. i is the control input for solenoid valve.

(b) Solenoid valve is also characterized by the electric equation:

$$V = Ri + i \frac{dL(x_v, i)}{dt} + L(x_v, i) \frac{di}{dt} \quad (14)$$

From the above equation, we can see that an inner loop to control current can be introduced to improve current input accuracy. According to (Malaguti et al., 2002), mechanical dynamics of solenoid valve is slow respect to electric one, so we obtain the simple electric equation.

$$V = Ri + L(x_{v0}) \frac{di}{dt} \quad (15)$$

The inductance is supposed constant in the operating position and independent on current. And specific values of valve's parameters can be found in (Liu H. et al., 2008).

2.4 Full State Mode

Assigning the states as $x_1 = z_s - z_u$, $x_2 = \dot{z}_s - \dot{z}_u$, $x_3 = z_u$, $x_4 = \dot{z}_u$, $x_5 = x_v$, $x_6 = \dot{x}_v$, $x_7 = i$, and combining all the equations we obtain the full state model.

$$\dot{x}_1 = x_2; \quad (16)$$

$$\dot{x}_2 = \frac{1}{m_u} (K_t x_3 + C_t x_4) - \frac{m_s + m_u}{m_s m_u} F; \quad (17)$$

$$\dot{x}_3 = x_4; \quad (18)$$

$$\dot{x}_4 = g + \frac{1}{m_u} [F - K_t x_3 - C_t x_4]; \quad (19)$$

$$\dot{x}_5 = x_6; \quad (20)$$

$$\dot{x}_6 = \frac{1}{m_v} [B(x_5) x_7^2 - C_s x_6 - (K_s + K_f) x_5 - f - f_0]; \quad (21)$$

$$\dot{x}_7 = \frac{1}{L} (V - R x_7); \quad (22)$$

where F , F_{air} and F_{oil} can be expressed as following,

$$F = (1 + K_m) F_{air} + F_{oil} \quad (23)$$

$$F_{air} = P_i A_a \left(\frac{V_0}{V_0 - A_a x_1} \right)^n - P_0 A_a \quad (24)$$

$$F_{oil} = \frac{\rho A_o^3 \operatorname{sgn}(x_2)}{2(K_v x_5 C_d)^2 \sqrt{1 - (K_v x_5 / A_o)^2}} x_2^2 \quad (25)$$

3. Design Objective of Oleopneumatic Shock Absorber in Landing Gear System

The tasks of aircraft landing gears are complex and lead to a number of sometimes contradictory requirements. At touchdown, the landing gear has to perform its task of absorbing the aircraft vertical energy via the shock absorber and the horizontal energy by the brakes. At taxiing, the landing gear has to carry the aircraft over taxiways and runways of varying quality. The requirements for absorption of a hard touch-down and for comfortable rolling lead to a design conflict.

3.1 Touchdown Phase

At touchdown phase, the design objective of oleo-pneumatic shock absorber is aimed at reducing the maximum vertical load level introduced at the fuselage attachment and producing a possibly "balanced" set of landing structural loads at touchdown. To get optimal structural load, the impact energy should be equally distributed with respect to the shock absorber stroke. So the optimal structural load during touchdown is a constant value:

$$F_{sao} = \frac{\int_0^{z_{cc}} F_{sa}(z) dz}{z_0} \quad (26)$$

F_{sao} can be estimated by the total energy to be absorbed at touchdown, including kinetic energy and potential energy in vertical direction, and the expected stroke of shock absorber which is generally 90%-95% of the maximal stroke (the work done by drag and lift are omitted).

It is hard for a conventional passive landing gear system to achieve this optimal target load. Semi-active landing gear system has a better performance due to its flexible structure, and is possible to reach the ideal effect if a suitable control method is used. Actually, stroke z_1 is needed to travel before structural load reaches F_{sao} , and this part of the gear compression cannot overly reduced (Ghiringhelli et al., 2004). If z_1 is too short, the gear stiffness will be large and thus the longitudinal spin-up loads will increase sharply. That will lead to the reduction of unitary efficiency. So a reasonable choice is to use passive control till the structural load reaches F_{sao} , and then change to semi-active control afterwards. That results F_{sas} , a sub-optimal structural load solution. By using this scheme, the unitary efficiency of a landing gear system can be achieved though the efficiency of the shock absorber is decreased.

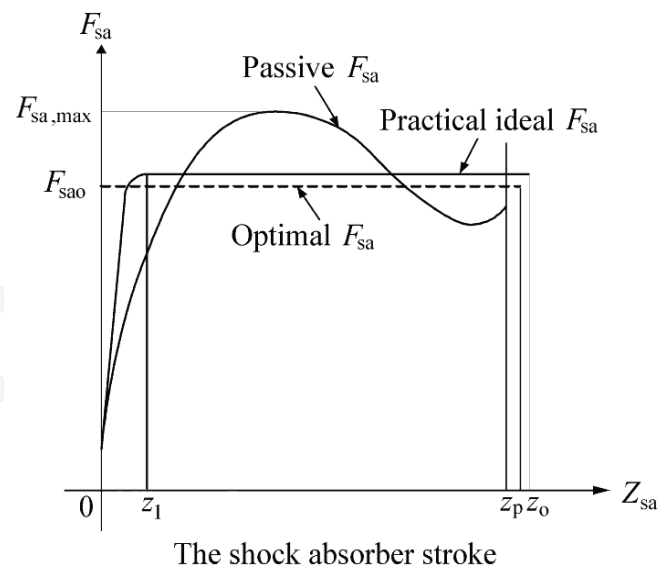


Fig. 4. Shock Absorber Efficiency Comparison

3.2 Taxiing Phase

At taxiing phase, the design objective of oleo-pneumatic shock absorber is aimed at filtering the unevenness of runway surface and providing a comfortable ground ride. It is expected that an aircraft rapidly returns to its original equilibrium state and have minimum vertical displacement when influenced by a runway excitation such as bump or cave. So the maximum vertical displacement of airframe over a test runway is an important criterion for shock absorber design. Another design criterion is root-mean-square (RMS) of airframe vertical acceleration by reason that ground induced vibrations become more and more of a problem as structures of modern aircraft become increasingly flexible. That will lead to shorten the fatigue life of the landing gear and of the airframe.

The RMS of acceleration is defined as follows

$$C_{RMS} = \sqrt{\frac{1}{t_e - t_0} \int_{t_0}^{t_e} (\ddot{z}_s - \ddot{z}_{sr})^2 dt} \quad (27)$$

with airframe's vertical acceleration \ddot{z}_s and reference value for acceleration evaluation \ddot{z}_{sr} .

3.3 Transition From Touchdown to Taxiing

The damping required to successfully encounter oscillations has to considerably larger for taxiing than for touchdown because the oleo stroke velocity at taxiing is significantly smaller than at touchdown. So there exists a transition between touchdown phase and taxiing phase. For passive landing gear, a standard solution is the use of a double-stage air spring or a taxi valve. At low stroke velocities (taxiing), high damping factor is achieved, while at high stroke velocity (touchdown), the valve reduces its damping factor. For our semi-active landing gear, the transition from touchdown phase to taxiing phase is also monitored by

measurement of stroke velocity and the damping factor of the shock absorber is changed by variable-sized oil orifice.

3.4 Dual Mode Controller

Due to totally different design goal of landing gear during aircraft touchdown phase and taxiing phase, the semi-active controller should be able to switch from one mode to another. Thus a dual mode predictive controller will be proposed in the following sections. Fig.5 shows the structure of the dual mode controller.

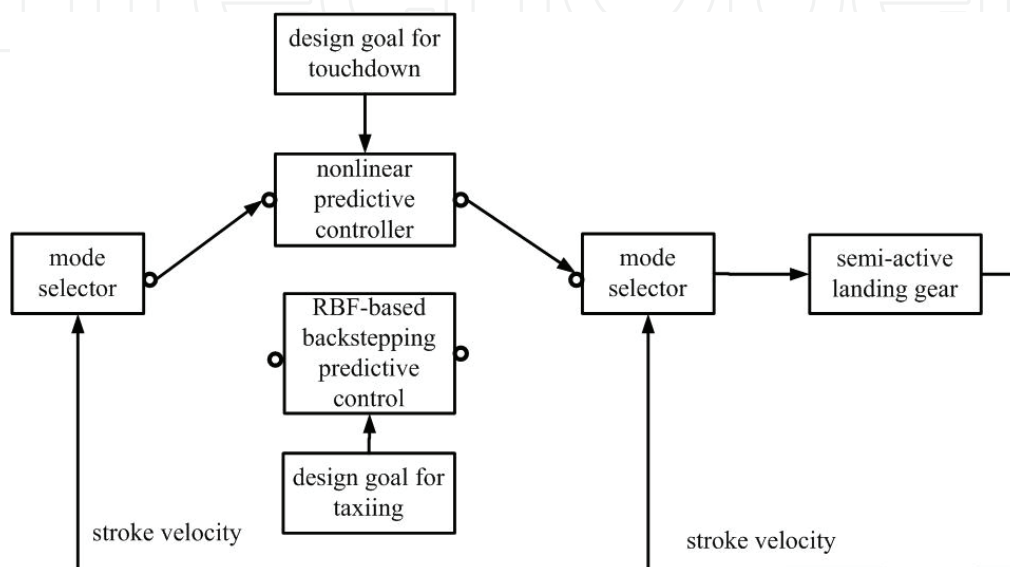


Fig. 5. Controller Switching Between Touchdown Phase and Taxiing Phase

4. Semi-Active Predictive Controller Design for Touchdown Phase

It is noted that the hydraulic dynamics, pneumatic dynamics and fast valve dynamics make controls design very difficult. In order to achieve the ideal objective, a proper semi-active control method should be applied. Considering the highly nonlinear behaviour of landing gear, the classical linear control theory will be useless. The advances of nonlinear control theory make it possible to transform certain types of nonlinear systems to linear system (Slotine et al., 1991).

4.1 Inverse Dynamics Controller

The semi-active landing gear dynamic model (eq.16-25) can be simplified as a following SISO nonlinear system:

$$\dot{x} = f(x) + g(x)u \quad (28)$$

$$y = c(x) \quad (29)$$

Where, u is the system input which stands for actuator's driving voltage V , y is the system output which stands for the shock absorber force F .

To deal with strong nonlinearities, generally an input-output linearization can be adopted during the system synthesis process. The basic approach of input-output linearization is simply differentiating the output function y repeatedly until the input u appears, and then designing u to cancel the nonlinearity (Slotine et al., 1991). However, the nonlinearity cancelling can not be carried out here because the relative degree of the semi-active landing gear system is undefined,

Since the semi-active landing gear dynamic model consists of shock absorber's model and high-speed solenoid valve's model, we propose a cascade nonlinear inverse dynamics controller. First, an expected oil orifice area A_d for the shock absorber is directly computed by inversion of nonlinear model if control valve's limited magnitude and rate are omitted,

$$A_d = \sqrt{\frac{\rho A_0^3}{2x_2^2 C_d^2 (F_{sao} - F_{air} - K_m F_{air})}} \quad (30)$$

Then a nonlinear tracking controller for high-speed solenoid valve can be designed to follow the expected movable parts position of solenoid valve. However, the practical actuator has magnitude and rate limitations. The maximum adjustable open area of the valve is 7.4mm^2 and switch frequency is 100Hz . So the optimal performance is not achievable.

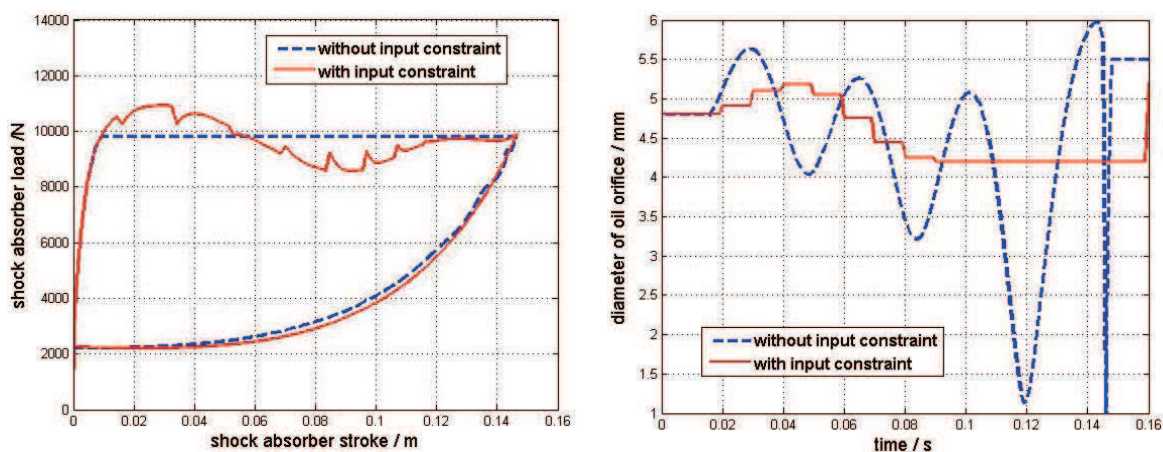


Fig. 6. Shock Absorber Efficiency and Control Input Comparison w/o Input Constraints

From the above figures, we can see that the high-speed solenoid valve's limited rate and magnitude have negative effects on the shock absorber if those input constraints are not considered during the controller synthesis process.

4.2 Nonlinear Predictive Controller

Model predictive control (MPC) is suitable for constrained, digital control problems. Initially MPC has been widely used in the industrial processes with linear models, but recently some researchers have tried to apply MPC to other fields like automotive and aerospace, and the nonlinear model is used instead of linear one due to the increasingly high demands on better control performance. However, optimization is a difficult task for nonlinear model predictive control (NMPC) problem. Generally a standard nonlinear programming method such as SQP is used. But it is the non-convex optimization method for constrained nonlinear

problem, thus global optimum can not be obtained. Furthermore, due to its high computational requirement, SQP method is not suitable for online optimization.

To the semi-active landing gear control problem, a nonlinear output-tracking predictive control approach (Lu, 1998) is adopted here considering its effectiveness to constrained control problems and real-time performance. The basic principle of this control approach is to get a nonlinear feedback control law by solving an approximate receding-horizon control problem via a multi-step predictive control formulation.

The nonlinear state equation and output equation are defined by eq. (28-29). And the following receding-horizon problem can be set up for providing the output-tracking control:

$$\min_u J[\mathbf{x}(t), t, u] = \min_u \frac{1}{2} \int_t^{t+T} [e^T(\tau) \mathbf{Q} e(\tau) + u^T(\tau) \mathbf{R} u(\tau)] d\tau \quad (31)$$

subject to the state equations (28) and

$$e(t+T) = 0 \quad (32)$$

where $e(t) = y(t) - y_d(t)$.

Then we shall approximate the above receding-horizon control problem by the following multi-step-ahead predictive control formulation. Define $h = T/N$, with N is control number during the prediction horizon. The output $y(t+kh)$ is approximated by the first-order Taylor series expansion

$$y(t+kh) \approx y(t) + \mathbf{C}[\mathbf{x}(t)] \{ \mathbf{x}(t+kh) - \mathbf{x}(t) \}, \quad 1 \leq k \leq N \quad (33)$$

where $\mathbf{C} = \partial \mathbf{c}(\mathbf{x}) / \partial \mathbf{x}$. The desired output $y_d(t+kh)$ is predicted similarly by recursive first-order Taylor series expansions

$$y_d(t+h) \approx y_d(t) + h\dot{y}_d(t)$$

$$y_d(t+2h) \approx y_d(t+h) + h\dot{y}_d(t+h) \approx y_d(t) + h\dot{y}_d(t) + h[\dot{y}_d(t) + h\ddot{y}_d(t)]$$

where another first-order expansion $\dot{y}_d(t+h) \approx \dot{y}_d(t) + h\ddot{y}_d(t)$, then we have

$$y_d(t+kh) \approx y_d(t) + h \left[\sum_{i=0}^{k-1} (1+hp)^i p y_d(t) \right] \quad (34)$$

where $p = d/dt$ is the differentiation operator. Combining the predictions of $y(t+kh)$ and $y_d(t+kh)$, we obtain the prediction of the tracking error

$$e(t+kh) = y(t+kh) - y_d(t+kh) \approx h \left\{ \sum_{i=0}^{k-1} [C(I+hF)^i] f + \sum_{i=0}^{k-1} [C(I+hF)^i g u(t+(k-1-i)h) - (1+hp)^i p y_d(t)] \right\} \quad (35)$$

where $F(\mathbf{x}) = \partial \mathbf{f}(\mathbf{x}) / \partial \mathbf{x}$. Approximating the cost function by the trapezoidal rule, it can be written as a quadratic function

$$\bar{J} = \frac{1}{2} \mathbf{v}^T \mathbf{H}(\mathbf{x}) \mathbf{v} + \mathbf{r}^T(\mathbf{x}) \mathbf{v} + \mathbf{q}(e, \mathbf{x}, y_d) \quad (36)$$

where $\mathbf{v} = \text{col}\{u(t), u(t+h), \dots, u[t+(N+1)h]\}$.

The constraint (eq. (32)) is then expressed as $e(t+Nh) = \mathbf{0}$ which leads to

$$\mathbf{M}^T(\mathbf{x}) \mathbf{v} = \mathbf{d}(e, \mathbf{x}, y_d) \quad (37)$$

where

$$\mathbf{M}^T = C[(I+hF)^{N-1} \mathbf{g}, \dots, (I+hF) \mathbf{g}, \mathbf{g}] \quad (38)$$

$$\mathbf{d} = -\frac{1}{h} e - \sum_{i=0}^{N-1} [C(I+hF)^i \mathbf{f} - (1+hp)^i p y_d(t)] \quad (39)$$

Now the output-tracking receding-horizon optimal control problem is reduced to the problem of minimizing \bar{J} with respect to \mathbf{v} subject to eq. (37), which is a quadratic programming problem. The closed-form optimal solution for this problem is

$$\mathbf{v} = -[\mathbf{H}^{-1} - \mathbf{H}^{-1} \mathbf{M}(\mathbf{M}^T \mathbf{H}^{-1} \mathbf{M})^{-1} \mathbf{M}^T \mathbf{H}^{-1}] \mathbf{r} + [\mathbf{H}^{-1} \mathbf{M}(\mathbf{M}^T \mathbf{H}^{-1} \mathbf{M})^{-1}] \mathbf{d} \quad (40)$$

Then the closed-loop nonlinear predictive output-tracking control law is

$$u(t; \mathbf{x}, N) = \mathbf{v}(1) \quad (41)$$

Unlike the input-output feedback linearization control laws, the existence of the proposed nonlinear predictive output-tracking control does not depend on the requirement that the system have a relative degree. And more important, the actuator's amplitude and rate constraints can be taken into account during the controller synthesis process.

4.3 Numerical Simulation

Based on the analysis described in previous sections, the numerical simulation of the semi-active landing gear system responses are derived using MATLAB environment. The prototype of the simulation model is a semi-active landing gear comprehensive

experimental platform we built, which can be reconfigured to accomplish tasks such as drop tests, taxi tests and shimmy tests. The sprung mass of this system is 405kg and the unsprung mass is 15kg. The other parameters of the simulation model can be found in (Wu et al, 2007). Fig.7 is the photo of the experiment system.



Fig. 7. Landing gear experiment platform

Three kinds of control methods including passive control, inverse dynamics semi-active control and nonlinear predictive semi-active control are used in the computer simulation. The fixed size of oil orifice for passive control is optimized manually under following parameters: sinking speed is 2 m/s and aircraft sprung mass is 405 kg. In the process of simulation, the sprung mass remains constant and the comparison is taken in terms of different sinking speed: 1.5 m/s, 2 m/s and 2.5 m/s. For passive control, the orifice size is fixed. From the Figs. 8-10 and Table 1, when system parameters such as sinking speed change, the control performance of the passive control decreases greatly, for the fixed orifice size in passive control is designed under standard condition.

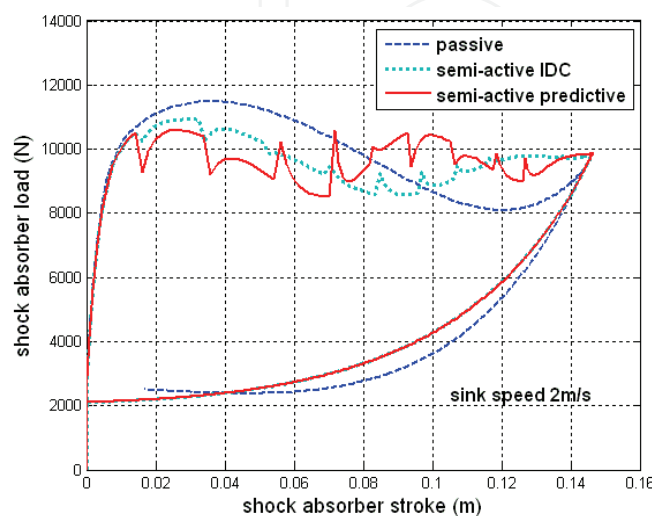


Fig. 8. Efficiency Comparison under Normal Condition

Conventional passive landing gear is especially optimized for heavy landing load condition, so the passive landing gear behaves even worse under light landing load condition. The performance of semi-active control is superior to that of passive one due to its tunable orifice size and nonlinear predictive semi-active control method has the best performance of all. Due to its continuous online compensation and consideration of actuator's constraints, nonlinear predictive semi-active control method can both increase the efficiency of shock absorber and make the output smoother during the control interval, which can effectively alleviate the fatigue damage of both airframe and landing gear.

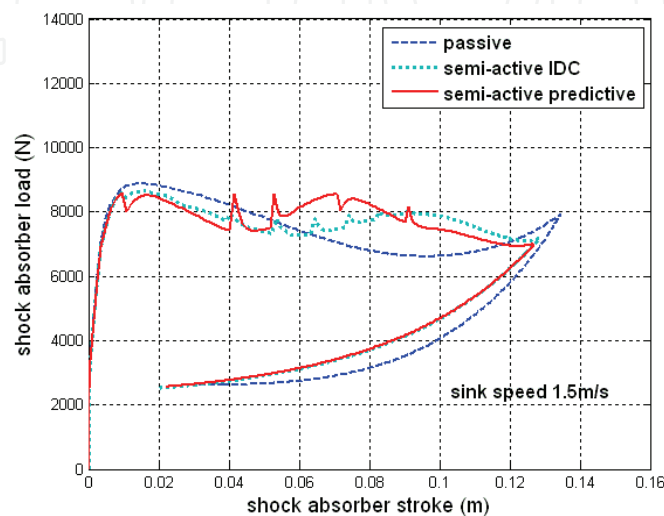


Fig. 9. Efficiency Comparison under Light Landing Load Condition

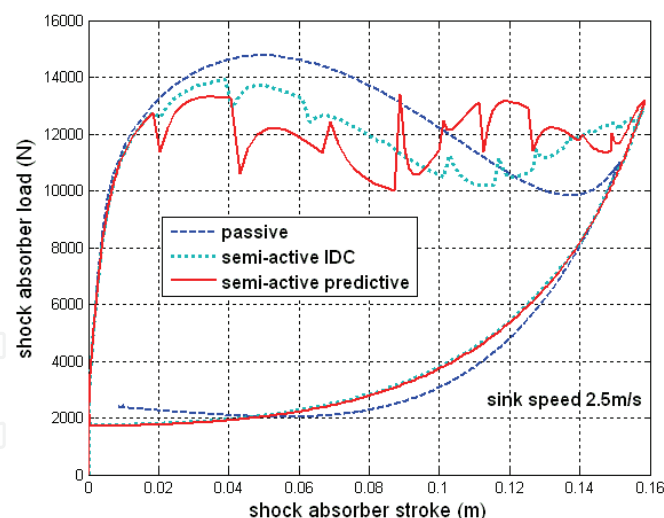


Fig. 10. Efficiency Comparison under Heavy Landing Load Condition

Control Method	Passive	Semi-Active IDC	Semi-Active Predictive
Efficiency/ $(2.0m \cdot s^{-1})$	0.8483	0.8788	0.9048
Efficiency/ $(1.5m \cdot s^{-1})$	0.8449	0.8739	0.9036
Efficiency/ $(2.5m \cdot s^{-1})$	0.8419	0.8554	0.8813

Table 1. Comparison of shock absorber efficiency

4.4 Sensitivity Analysis

Sometimes system parameters such as sinking speed, sprung weight and attitude of aircraft at touch down may be measured or estimated with errors, which will lead to bias of estimation for optimal target load. But the controller should behave robust to withstand certain measurement or estimation errors within reasonable scope so that the airframe will not suffer from large vertical load at touch down.

Simulation of sensitivity analysis is conducted under the standard condition controller design: sinking speed is 2 m/s and aircraft sprung mass is 405 kg, introducing 10% errors for sinking speed and sprung mass individually. The actual sinking speed is measured by avionic equipments and the aircraft sprung mass is estimated by considering the weights of oil, cargo and passengers. The measurement and estimation errors will be less than the assumed maximal one.

From the above Figs.11,12 simulation results, it can be seen that the reasonable measuring error of sinking speed has little effect on the performance of nonlinear predictive semi-active controller, whilst estimating error of sprung mass has side effect to the control performance and shock absorber efficiency decreases a little. To further improve the performance under mass estimating error, it is possible to either simply introduce measurement of aircraft mass or develop robust controller which is non-sensitive to estimating the error of aircraft sprung mass.

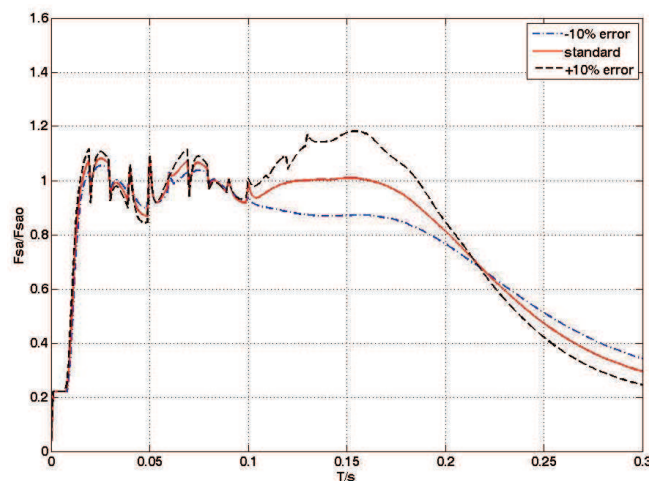


Fig. 11. Sensitivity to sink speed measuring error

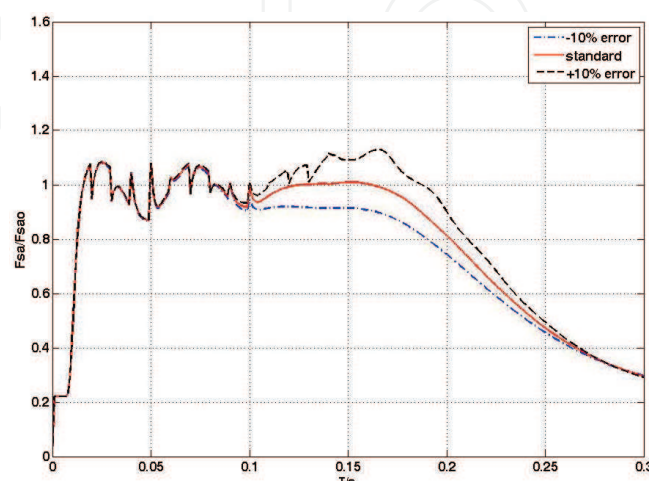


Fig. 12. Sensitivity to sprung mass estimating error

5. Semi-Active Predictive Controller Design for Taxiing Phase

In this section, we will propose a nonlinear predictive controller incorporating radial basis function network (RBF) and backstepping design methodology (Krstic et al., 1995) for semi-active controlled landing gear during aircraft taxiing.

5.1 Hierarchical Controller Structure

A hierarchical control structure which contains three control loops is adopted here. The outer loop determines the expected strut force of the semi-active shock absorber. At touchdown phase and taxiing phase, the computation of the expected strut force will be different due to different design objective. The middle loop is responsible for controlling of solenoid valve's mechanical and magnetic dynamics. The high speed solenoid valve contains high nonlinearity and can not be regulated by traditional linear controller i.e. PID. We develop a RBF network to approximate the nonlinear dynamics which can not be precisely modelled and adopt backstepping, a constructive nonlinear control design method to stabilize the whole nonlinear system. The inner loop is the current loop. It ensures stable tracking of commanded current that middle loop outputs.

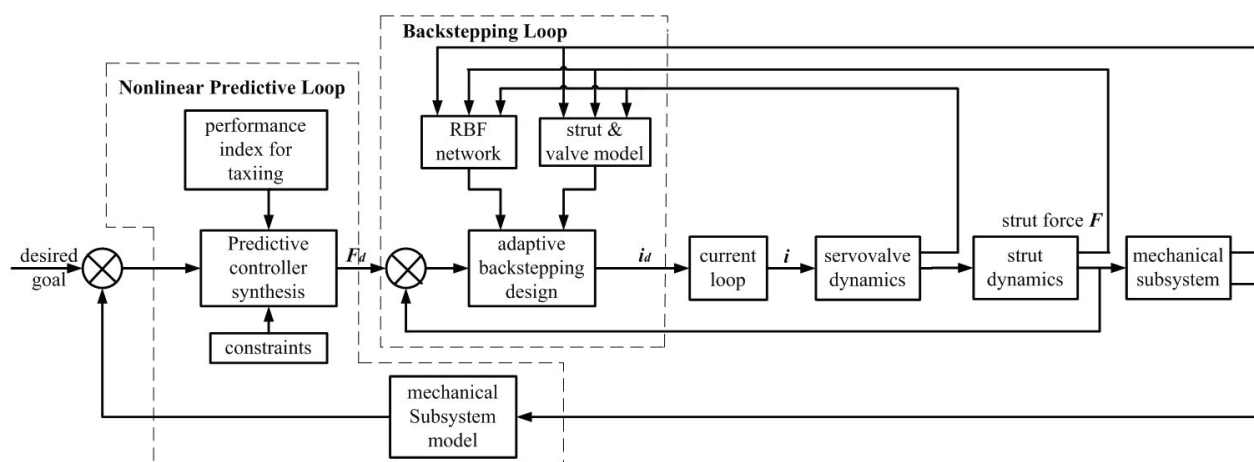


Fig. 13. Hierarchical Controller Structure

5.2 Background for RBF network

A RBF network is typically comprised of a layer of radial basis activation functions with an associated Euclidean input mapping. The output is then taken as a linear activation function with an inner product or weighted average input mapping.

In this paper, we use a weighted average mapping in the output node. The input-output relationship in a RBF with $\mathbf{x} = [x_1, \dots, x_n]^T$ as an input is given by

$$\Psi(\mathbf{x}, \boldsymbol{\theta}) = \frac{\sum_{i=1}^m w_i \exp(-|\mathbf{x} - c_i|^2 / \gamma^2)}{\sum_{i=1}^m \exp(-|\mathbf{x} - c_i|^2 / \gamma^2)} = \boldsymbol{\theta}^T \boldsymbol{\xi}(\mathbf{x}) \quad (42)$$

where

$$\boldsymbol{\theta} = [w_1, \dots, w_n]^T \quad (43)$$

$$\xi_i = \frac{\exp(-|\mathbf{x} - c_i|^2 / \gamma^2)}{\sum_{i=1}^m \exp(-|\mathbf{x} - c_i|^2 / \gamma^2)} \quad (44)$$

The RBF network is a good approximator for general nonlinear function. For a nonlinear function FN, we can express it using RBF network with the following form,

$$F_N = \boldsymbol{\theta}^T \boldsymbol{\xi} + \varepsilon = \hat{\boldsymbol{\theta}}^T \boldsymbol{\xi} + \tilde{\boldsymbol{\theta}}^T \boldsymbol{\xi} + \varepsilon \quad (45)$$

where $\boldsymbol{\theta}$ is the vector of tunable parameters under ideal approximation condition, $\hat{\boldsymbol{\theta}}$ under practical approximation condition, $\tilde{\boldsymbol{\theta}}$ parameter approximation error, ε function reconstruction error.

5.3 Outer Loop Design

The function of the outer control loop is to produce a target strut force for semi-active shock absorber by using active control law. Then middle loop and inner loop controller will be designed to approximate the optimal performance that active controller achieves.

(a) Skyhook Controller

At the taxiing phase, the landing gear system acts like the suspension of ground vehicle. So we first adopt the most widely used active suspension control approach - the skyhook controller. At this control scheme the actuator generates a control force which is proportional to the sprung mass vertical velocity. The equation of skyhook controller can be expressed as the following form:

$$F_{sky} = K_{sky}(x_{1d} - x_1) - C_{sky}(x_2 + x_4) \quad (46)$$

In order to blend out low frequency components of the vertical velocity signal which results from the aircraft taxiing on sloped runways or long bumps, we modify it by adding high pass filter to the skyhook controller.

$$x_s = \frac{s}{s + w_k} x_1 \quad (47)$$

where w_k is roll off frequency of high pass filter. Thus we get the desired strut force.

$$F_d = K_{sky}(x_{1d} - x_1) - C_{sky}(x_2 + x_4) - K_{HP}x_s \quad (48)$$

where K_{HP} is a constant scale factor.

(b) Nonlinear Predictive Controller

Compare with traditional skyhook controller, model predictive controller is more suitable for constrained nonlinear system like landing gear system or suspension system. Input and state constraints can be incorporated into the performance index to achieve best performance.

The system model of outer loop controller is eq. (16-19), which can be expressed as follows:

$$\dot{\mathbf{x}}_a = \mathbf{f}(\mathbf{x}_a) + \mathbf{g}(\mathbf{x}_a)F_d \quad (49)$$

where $\mathbf{x}_a = [x_1, x_2, x_3, x_4]$, F_d is the control input and the output equation is $y = x_1$. Then a similar receding-horizon problem can be set up for providing the output-tracking control:

$$\min_{F_d} J[\mathbf{x}_a(t), t, F_d] = \min_{F_d} \frac{1}{2} \int_t^{t+T} [e_a^T(\tau) \mathbf{Q}_a e_a(\tau) + F_d^T(\tau) \mathbf{R}_a F_d(\tau)] d\tau \quad (50)$$

subject to the state equations (49) and

$$e_a(t+T) = 0 \quad (51)$$

where $e_a(t) = x_1(t) - x_{1d}(t)$.

Following a similar synthesis process as in section 4.2, we can get a closed-loop nonlinear predictive output-tracking control law to achieve approximate optimal active control performance.

5.4 RBF-based Backstepping Design (Middle Loop)

In this section we propose a RBF-based backstepping method to complete the design of the semi-active controller. Stability proofs are given.

First we define the force tracking error as $e_1 = F_d - F$. Differentiate and substitute from Eq. (16-25),

$$\begin{aligned} \dot{e}_1 &= \dot{F}_d - \dot{F} = \dot{F}_d - \frac{d}{dt} [(1+K_m)F_{air} + F_{oil}] \\ &= \dot{F}_d - \frac{d}{dx_5} \left(\frac{\rho A_o^3}{2(K_v x_5 C_d)^2 \sqrt{1 - (K_v x_5 / A_o)^2}} \right) x_2^2 \dot{x}_5 \\ &\quad - \frac{\rho A_o^3}{(K_v x_5 C_d)^2 \sqrt{1 - (K_v x_5 / A_o)^2}} x_2 \dot{x}_2 \\ &\quad - (1+K_m) \frac{d}{dx_1} \left[P_i A_a \left(\frac{V_0}{V_0 - A_a x_1} \right)^n - P_0 A_a \right] \dot{x}_1 \\ &= \dot{F}_d + G_1(x_2, x_5) x_6 + H_1(x_1, x_2, x_3, x_4, x_5) \end{aligned}$$

where $G_1(x_2, x_5)$, $H_1(x_1, x_2, x_3, x_4, x_5)$ is the nonlinear functions related to the strut dynamics.

(a) First Step

Select the desired solenoid valve movable part velocity as

$$x_{6d} = -G_1^{-1}(H_1 + \dot{F}_d + k_1 e_1) \quad (52)$$

where k_1 is a design parameter. Then we get

$$\begin{aligned} \dot{e}_1 &= \dot{F}_d + G_1(x_2, x_5)x_{6d} + G_1(x_2, x_5)e_2 + H_1(x_1, x_2, x_3, x_4, x_5) \\ &= \dot{F}_d + G_1 e_2 - (H_1 + \dot{F}_d + k_1 e_1) + H_1 = G_1 e_2 - k_1 e_1 \end{aligned}$$

where $e_2 = x_6 - x_{6d}$.

Consider the following Lyapunov function candidate

$$V_1 = \frac{1}{2} e_1^2$$

Differentiate V_1 , thus we get

$$\dot{V}_1 = e_1 \dot{e}_1 = e_1 G_1 e_2 - k_1 e_1^2$$

(b) Second Step

x_6 is not the true control input. We then choose $u = x_7^2$ as virtual input.

Differentiate e_2 , we get

$$\dot{e}_2 = \dot{x}_6 - \dot{x}_{6d} = G_2 u - \frac{C_s}{m_v} x_6 + H_2 + W$$

where $G_2 = B(x_5)/m_v$, $H_2 = -f/m_v - \dot{x}_{6d}$ and $W = -[(K_s + K_f)x_5 + f_0]/m_v$.

Consider the following Lyapunov function candidate

$$V_2 = V_1 + \frac{1}{2} e_2^2 + \frac{1}{2} \text{tr}(\tilde{\theta}_1^T \Gamma_1^{-1} \tilde{\theta}_1) + \frac{1}{2} \text{tr}(\tilde{\theta}_2^T \Gamma_2^{-1} \tilde{\theta}_2)$$

where Γ_1 and Γ_2 are positive definite matrices. Differentiate V_2

$$\dot{V}_2 = \dot{V}_1 + e_2 (G_2 u - \frac{C_s}{m_v} x_6 + H_2 + W) + \text{tr}(\tilde{\theta}_1^T \Gamma_1^{-1} \dot{\tilde{\theta}}_1) + \text{tr}(\tilde{\theta}_2^T \Gamma_2^{-1} \dot{\tilde{\theta}}_2)$$

Then we choose the control input:

$$u = -\hat{G}_2^{-1}(\hat{H}_2 - \frac{C_s}{m_v} x_{6d} + W + k_2 e_2 + G_1 e_1) \quad (53)$$

where k_2 is a design parameter, $\hat{G}_2 = \hat{\theta}_1^T \xi_1$ is the estimation of $G_2(x_2, x_5)$, $\hat{H}_2 = \hat{\theta}_2^T \xi_2$ is the estimation of $H(x_1, x_2, x_3, x_4, x_5)$. Thus we get

$$\begin{aligned} \dot{V}_2 &= \dot{V}_1 + e_2 \tilde{G}_2 u + e_2 \varepsilon_1 u - \frac{C_s}{m_v} e_2 + e_2 \tilde{H}_2 + e_2 \varepsilon_2 - e_2 k_2 e_2 - e_2 G_1 e_1 + \text{tr}(\tilde{\theta}_1^T \Gamma_1^{-1} \dot{\tilde{\theta}}_1) + \text{tr}(\tilde{\theta}_2^T \Gamma_2^{-1} \dot{\tilde{\theta}}_2) \\ &= \dot{V}_1 + e_2 \tilde{\theta}_1^T \xi_1 u + e_2 \tilde{\theta}_2^T \xi_2 - \tilde{\theta}_1^T \xi_1 u e_2 - \tilde{\theta}_2^T \xi_2 e_2 - e_2 k_2 e_2 - \frac{C_s}{m_v} e_2 + e_2 \varepsilon_1 u + e_2 \varepsilon_2 - e_2 G_1 e_1 \\ &\quad + \text{tr}[\tilde{\theta}_1^T (\Gamma_1^{-1} \dot{\tilde{\theta}}_1 + \xi_1 u e_2)] + \text{tr}[\tilde{\theta}_2^T (\Gamma_2^{-1} \dot{\tilde{\theta}}_2 + \xi_2 e_2)] \end{aligned}$$

Choose the tuning law as:

$$\dot{\hat{\theta}}_1 = -\Gamma_1 \xi_1 u e_2, \quad \dot{\hat{\theta}}_2 = -\Gamma_2 \xi_2 e_2 \quad (54)$$

So we have

$$\begin{aligned} \dot{V}_2 &= e_1 G_1 e_2 - k_1 e_1^2 - k_2 e_2^2 - e_2 G_1 e_2 - \frac{C_s}{m_v} e_2 + e_2 \varepsilon_1 u + e_2 \varepsilon_2 \\ &= -k_1 e_1^2 - k_2 (e_2 - \frac{\varepsilon_1 u + \varepsilon_2 - C_s/m_v}{2k_2})^2 - \frac{(\varepsilon_1 u + \varepsilon_2 - C_s/m_v)^2}{4k_2} \leq 0 \end{aligned}$$

Therefore, the system is stable and the error will asymptotically converge to zero.

5.5 Inner Loop Design

The function of the inner loop is to precisely tracking of solenoid valve's current. We apply a simple proportional control to the electrical dynamics as follows

$$V = K_c (x_{7d} - x_7) = K_c (\sqrt{u} - x_7) \quad (55)$$

where K_c is the controller gain.

The above three control loops represent different time scales. The fastest is the inner loop due to its electrical characteristics. The next is the middle loop. It is faster than the outer loop because the controlled moving part's inertial of the middle loop is much smaller than that of the outer loop.

5.6 Numerical Simulation

After touchdown, the taxiing process will last relatively a long time before aircraft stops. To simulate the road excitation of runway and taxiway, a random velocity excitation signal $w(t)$ is introduced into Eq. (18).

$$\dot{x}_3 = x_4 + w(t) \quad (56)$$

The simulation result is compared using airframe vertical displacement, which is one of the most important criterion for taxiing condition. Due to lack of self-tuning capability, the passive landing gear does not behave well and passes much of the road excitation to the airframe. That will be harmful for the aircraft structure and meanwhile make passages uncomfortable. The proposed semi-active landing gear effectively filters the unfriendly road excitation as we wish.

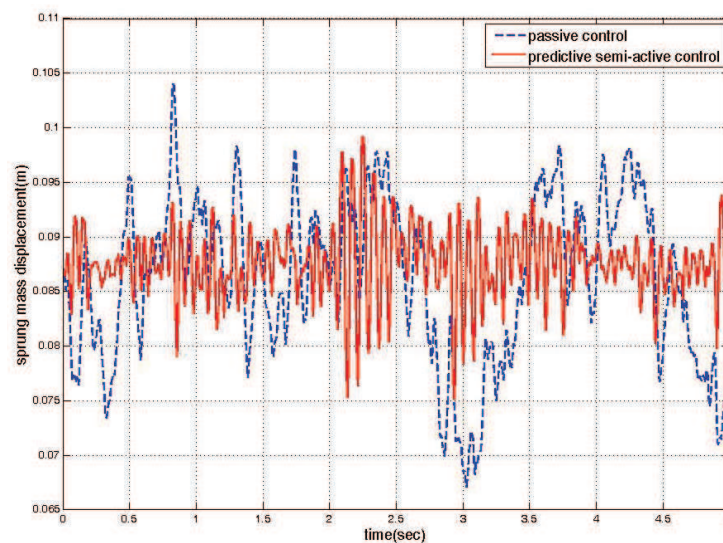


Fig. 14. System Response Comparison under Random Input

From the simulation results of both aircraft touch-down and taxiing conditions, we can see that the proposed semi-active controller gives the landing gear system extra flexibility to deal with the unknown and uncertain external environment. It will make the modern aircraft system being more intelligent and robust.

6. Conclusion

The application of model predictive control and constructive nonlinear control methodology to semi-active landing gear system is studied in this paper. A unified shock absorber mathematical model incorporates solenoid valve's electromechanical and magnetic dynamics is built to facilitate simulation and controller design. Then we propose a hierarchical control structure to deal with the high nonlinearity. A dual mode model predictive controller as an outer loop controller is developed to generate the ideal strut force on both touchdown and taxiing phase. And a systematic adaptive backstepping design method is used to stabilize the whole system and track the reference force in the middle and inner loop. Simulation results show that the proposed control scheme is superior to the traditional control methods.

7. References

- Batterbee, D.; Sims, N. & Stanway, R. (2007). Magnetorheological landing gear: 1. a design methodology. *Smart Materials and Structures*, Vol. 16, pp. 2429-2440.
- Ghiringhelli, L. G. (2000). Testing of semiactive landing gear control for a general aviation aircraft. *Journal of Aircraft*, Vol.7, No.4, pp.606-616.
- Ghiringhelli, L. G. & Gualdi, S. (2004). Evaluation of a landing gear semi-active control system for complete aircraft landing. *Aerotecnica Missili e Spazio*, No. 6, pp. 21-31.
- Hyochoong, B. & Choong-Seok, O. (2004). Predictive control for the attitude maneuver of a flexible spacecraft. *Aerospace Science and Technology*, Vol. 8, No. 5, pp. 443-452.
- Karnopp, D. (1983). Active damping in road vehicle suspension systems. *Vehicle System Dynamics*, Vol.12, No. 6, pp.291-316.
- Kristic, M.; Kanellakopoulos, I. & Kokotovic, P.V. (1995). *Nonlinear and Adaptive Control Design*, Wiley-Interscience, ISBN: 978-0-471-12732-1, USA.
- Krüger, W. (2000). Integrated design process for the development of semi-active landing gears for transport aircraft, PhD thesis, University of Stuttgart.
- Liu, H.; Gu, H. B. & Chen, D. W. (2008). Application of high-speed solenoid valve to the semi-active control of landing gear. *Chinese Journal of Aeronautics*, Vol.21, No.3, pp.232-240.
- Liu, H. & Gu, H. B. (2008). Nonlinear model for a high-speed solenoid valve and its simulation. *Mechanical Science and Technology for Aerospace Engineering*, Vol.27, No.7, pp.866-870.
- Lou, Z.; Ervin, R. & Winkler, C. (1993). An electrorheologically controlled semi-active landing gear. SAE Paper931403.
- Lu, P. (1998). Approximate nonlinear receding-horizon control laws in closed form. *International Journal of Control*, Vol. 71, No.1, pp.19-34.
- Maemori, K.; Tanigawa, N. & Koganei R (2003). Optimization of a semi-active shock absorber for aircraft landing gear, *Proceedings of ASME Design Engineering Technical Conference*, pp.597-603.
- Malaguti, F. & Pregolato, E. (2002). Proportional control of on/off solenoid operated hydraulic valve by nonlinear robust controller, *Proceedings of IEEE International Symposium on Industrial Electronics*, pp.415-419.
- Mehra, R. K.; Amin, J. N. & Hedrick, K. J. (1997). Active suspension using preview information and model predictive control, *Proceedings of the 1997 IEEE International Conference on Control Applications*, pp. 860-865.
- Michael, A. H. (1998). Nonlinear model predictive control: current status and future direction. *Computers and Chemical Engineering*, Vol.23, pp.187-202.
- Mikulowski, G. & LeLetty, R. (2008). Advanced landing gears for improved impact absorption, *Proceedings of the 11th International conf. on New Actuators*, pp.175-194.
- Slotine, J.E. & Li, W.P. (1991). *Applied Nonlinear Control*, Prentice Hall, ISBN: 0-13-040890-5, USA.
- Wang, X. M. & Carl U. (1999). Fuzzy control of aircraft semi-active landing gear system, *AIAA 37th Aerospace Sciences Meeting and Exhibit*.
- Wu, D. S.; Gu, H.B.; Liu, H. (2007). GA-based model predictive control of semi-active landing gear. *Chinese Journal of Aeronautics*, Vol.20, No.1, pp.47-54.
- Yadav, D. & Ramamoorthy, R. P. (1991). Nonlinear landing gear behavior at touchdown. *Journal of Dynamic Systems, Measurement and Control*, Vol.113, No.12, pp.677-683.



Model Predictive Control

Edited by Tao Zheng

ISBN 978-953-307-102-2

Hard cover, 304 pages

Publisher Sciyo

Published online 18, August, 2010

Published in print edition August, 2010

Frontiers of Model Predictive Control Robust Model Predictive Control Nonlinear Model Predictive Control
Excellent Applications Guide for Researchers and Engineers Recent Achievements of Authors over the World
Theory with Practical Examples Kinds of Algorithms for Choice

How to reference

In order to correctly reference this scholarly work, feel free to copy and paste the following:

Dongsu Wu, Hongbin Gu and Hui Liu (2010). Nonlinear Predictive Control of Semi-Active Landing Gear System, Model Predictive Control, Tao Zheng (Ed.), ISBN: 978-953-307-102-2, InTech, Available from: <http://www.intechopen.com/books/model-predictive-control/nonlinear-predictive-control-of-semi-active-landing-gear-system>

INTECH
open science | open minds

InTech Europe

University Campus STeP Ri
Slavka Krautzeka 83/A
51000 Rijeka, Croatia
Phone: +385 (51) 770 447
Fax: +385 (51) 686 166
www.intechopen.com

InTech China

Unit 405, Office Block, Hotel Equatorial Shanghai
No.65, Yan An Road (West), Shanghai, 200040, China
中国上海市延安西路65号上海国际贵都大饭店办公楼405单元
Phone: +86-21-62489820
Fax: +86-21-62489821

© 2010 The Author(s). Licensee IntechOpen. This chapter is distributed under the terms of the [Creative Commons Attribution-NonCommercial-ShareAlike-3.0 License](#), which permits use, distribution and reproduction for non-commercial purposes, provided the original is properly cited and derivative works building on this content are distributed under the same license.

IntechOpen

IntechOpen